Vol. 13: 285–294, 1997 | AQUATIC MICROBIAL ECOLOGY Aquat Microb Ecol | Published September 11

Anoxic aggregates — an ephemeral phenomenon in the pelagic environment?

Helle Ploug*, Michael Kühl, Berit Buchholz-Cleven, Bo Barker Jørgensen

Max Planck Institute for Marine Microbiology, Celsiusstr. 1, D-28359 Bremen, Germany

ABSTRACT: Radial microscale distributions of oxygen and pH were studied in ca 1.5 mm large laboratory-made aggregates composed of phytoplankton detritus and fecal pellets. Microsensor measurements were done at spatial increments down to 0.05 mm in a vertical flow system in which the individual aggregates stabilized their position in the water phase according to the upward flow velocity. The aggregates were surrounded by a diffusive boundary layer with steep gradients of oxygen and pH. They were highly heterotrophic communities both under natural light conditions and in darkness. pH was lowered from 8.2 in the surrounding water to 7.4 in the center of an anoxic aggregate. Sulfide was not detectable by use of sulfide microelectrodes in anoxic aggregates, and methanogenic bacteria could not be detected after PCR (polymerase chain reaction) amplification using archaebacterial-specific primers. The oxygen respiration rate decreased exponentially over time with a $T_{1/2}$ of 2.3 d. Theoretical calculations of the volumetric oxygen respiration rate needed to deplete oxygen inside aggregates was compared to the density of organic matter in natural marine aggregates. These calculations showed that carbon limitation of heterotrophic processes would limit anoxic conditions to occurring only over a few hours, depending on the size of the aggregates. Therefore slow-growing obligate anaerobic microorganisms such as sulfate reducing bacteria and methanogenic bacteria may be limited by the relatively short persistence of anoxia in marine aggregates.

KEY WORDS: Microelectrodes · Molecular techniques · Diffusive boundary layers · Modeling

INTRODUCTION

A significant portion of suspended matter in the sea and in lakes exists in the form of rapidly sinking aggregates comprised of phytoplankton and other microorganisms, of organic detritus, zooplankton fecal pellets and inorganic particles (Alldredge & Silver 1988). The degradation of phytoplankton detritus aggregates is characterized by a microbial succession involving heterotrophic bacteria and bacteriovorous protozoa (Biddanda 1988, Biddanda & Pomeroy 1988). Although aggregates can reach sizes up to 75 mm in maximum length (Alldredge & Gotschalk 1988), it is not evident from direct measurements by microelectrodes if anoxia develops during the concurrent decay and sedimentation processes of marine snow comprised of diatoms (Alldredge & Cohen 1987). Anoxia has, however, been measured in a several millimeter large crustacean fecal pellet with an intact peritrophic membrane (Alldredge & Cohen 1987). Anoxic microenvironments harboring strictly anaerobic bacteria have been suggested as a source for the observed methane production in oxygenated waters (Lamontagne et al. 1973, Sieburth 1993). Low redox potentials measured by the use of tetrazolium salts and sulfide measured spectrophotometrically have suggested that sulfate reduction occurs in marine snow (Shanks & Reeder 1993). Isolation of strictly anaerobic bacteria from fresh zooplankton fecal pellets and large aggregates with numerous large fecal pellets from sediment traps (Bianchi et al. 1992) and measurements of methane fluxes associated with sediment trap material (Karl & Tilbrook 1994) have shown that anoxic microenvironments may be present in zooplankton guts and/or sinking zooplankton fecal pellets (Karl & Tilbrook 1994, Tilbrook & Karl 1995).

Here we present direct measurements of anoxic conditions in freely sinking aggregates composed of phytoplankton detritus and fecal pellets surrounded by fully oxygenated seawater. The volumetric oxygen res-

*E-mail: hploug@mpi-bremen.de

© Inter-Research 1997

Table 1. List of symbols and their definitions

C (nmol cm^{-3})	Concentration
C_r (nmol cm^{-3})	Concentration at the radial distance, r
C_0 (nmol cm^{-3})	Concentration at the surface, r_0
C_∞ (nmol cm^{-3})	Bulk water concentration
D (cm^2 s^{-1})	Molecular diffusion coefficient
D_{agg} (cm^2 s^{-1})	Effective diffusion coefficient in an aggregate
D_w (cm^2 s^{-1})	Molecular diffusion coefficient in seawater
$\delta_{eff.}$ (cm)	Effective diffusive boundary layer thickness
E (s^{-1})	Shear rate
ε (cm^2 s^{-3})	Energy dissipation rate
k_c (cm s^{-1})	Mass transport coefficient
K_m (µM)	Half-saturation constant
J (nmol cm^{-2} s^{-1})	Diffusive flux
n (cm^{-2} s^{-1})	Kinematic viscosity
R (nmol cm^{-3} s^{-1})	Volumetric respiration rate
r_0 (cm)	Surface radius
r_c(cm)	Radius at which the O_2 concentration is zero
r (cm)	Radius
Sh (dimensionless)	Sherwood number
U (cm s^{-1})	Sinking velocity
Q (nmol s^{-1})	Area-integrated diffusive flux

piration rates and carbon turnover times in anoxic aggregates are analyzed with respect to the carbon content in naturally occurring aggregates of marine snow and fecal pellets.

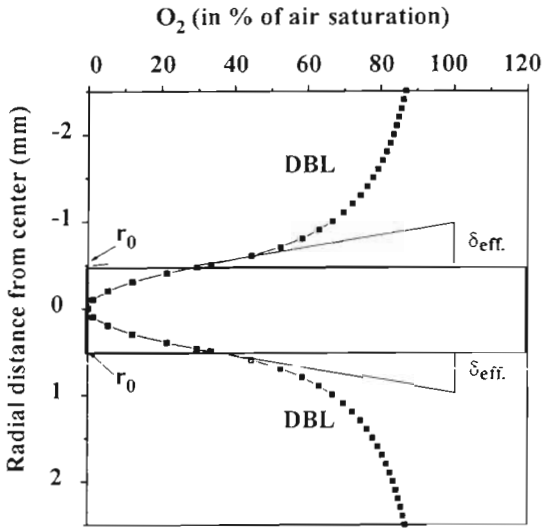

Fig. 1 A hypothetical (see text), radial oxygen distribution in the diffusive boundary layer (DBL) and within a 1 mm spherical aggregate (shaded area), which is anoxic exactly at the center under stagnant conditions. The effective DBL thickness, $\delta_{eff.}$, is shown

MATERIAL AND METHODS

Theoretical calculations. ***Diffusive boundary layers:*** When mass transfer to a sphere proceeds only by molecular diffusion, e.g. in a diffusive boundary layer (DBL) at the sphere-water interface, the concentration, C_r, at the radial distance, r, within the DBL can be described by (Crank 1975):

$$C_r = \frac{C_0 r_0 (r_1 - r) + C_1 r_1 (r - r_0)}{r(r_1 - r_0)} \quad (1)$$

where C_0 is the concentration at the surface, r_0, C_1 is the concentration at the radial distance r_1, and $r_0 < r < r_1$.

The radial flux of oxygen is expressed by Fick's first law of diffusion:

$$J = -D_w \frac{dC}{dr} \quad (2)$$

where J is the flux of oxygen per surface area, D_w is the molecular diffusion coefficient of oxygen in seawater. A list of symbols is shown in Table 1. The area-integrated flux per unit time, Q_t, through the DBL is described by (Crank 1975):

$$Q_t = 4\pi D_w \frac{r_0 r_1}{r_1 - r_0}(C_1 - C_0) \quad (3)$$

A hypothetical example of the radial oxygen distribution inside and around a 1 mm aggregate which is anoxic at the very center under stagnant conditions (r_1 tends to ∞) is shown in Fig. 1. Regarding the DBL as an array of concentric shells, the surface area of each shell increases with r^2. As the flux per surface area is proportional to the radial gradient through each concentric shell, the radial gradient therefore decreases with r^2 without a decrease in the (total) area-integrated flux. The DBL thickness can thus be determined from the curvature of the oxygen profile as the largest radial distance which yields the same total flux in the water phase as the total flux at the sphere surface, r_0.

In mass transfer theory, DBLs have been replaced by the mass transfer coefficient, k_c, which equals the ratio between the diffusion coefficient, D_w, and the effective (or hypothetical) DBL thickness, $\delta_{eff.}$. The $\delta_{eff.}$ is defined by extrapolating the radial oxygen gradient at the sphere-water interface, r_0, to the bulk water phase concentration. Thus,

$$J = -D_w \frac{C_\infty - C_0}{\delta_{eff.}} = -k_c (C_\infty - C_0) \quad (4)$$

where k_c is the mass transport coefficient, which equals $D_w/\delta_{eff.}$. It should be noticed that this extrapolation yields the same flux as Eq. (2). The mass transport coefficient increases with increasing flow, due to a decrease in the DBL thickness.

The Sherwood number, *Sh*, describes the increase in mass transfer due to flow (Sherwood et al. 1975). In a stagnant fluid:

$$Sh = \frac{k_c r_0}{D_w} = 1 \quad (5)$$

where r_0 is the radius of the sphere. However, as k_c equals the ratio of the diffusion coefficient and the effective DBL thickness, δ_{eff} (Sherwood et al. 1975):

$$Sh = \frac{r_0}{\delta_{eff}} = 1 \quad (6)$$

Whereas the real DBL is infinite in a stagnant fluid, a hypothetical DBL, $\delta_{eff.}$, which yields an equivalent flux of mass transfer to a sphere, thus extends to a distance outside the sphere which is equal to the radius of the sphere, as shown in Fig. 1. This hypothetical boundary layer decreases inversely proportional to *Sh* for sinking spheres or in a turbulent environment.

Concentration gradients within a sphere: The flux of oxygen and, thus, the radial gradient of oxygen decreases towards the center of an aggregate, as oxygen is consumed within the aggregate. At steady state, the oxygen concentration inside a sphere with zero order oxygen consumption and spherical diffusion is described by (Jørgensen 1977):

$$C_r = -\frac{R}{6D_{agg}}(r_0^2 - r^2) + C_0 \quad (7)$$

where $D_{agg.}$ is the effective diffusion coefficient of oxygen in the aggregate and R is the volumetric respiration rate.

The concentration at the surface, C_0, is dependent on the volumetric oxygen respiration rate in the aggregate, as the area-integrated flux of oxygen through the DBL at steady state is equal to the total oxygen being consumed within the aggregate. Assuming an evenly distributed oxygen consumption and that anoxia does not occur, the volumetric oxygen respiration rate is, therefore, described by:

$$R = \frac{4\pi r_0^2}{\frac{4}{3}\pi r_0^3}\frac{D_w(C_\infty - C_0)}{\delta_{eff.}} = \frac{3D_w}{r_0\,\delta_{eff.}}(C_\infty - C_0) \quad (8)$$

where $4\pi r_0^2$ and $\frac{4}{3}\pi r_0^3$ are the surface area and volume, respectively, of a sphere.

C_0 decreases linearly with an increase in the oxygen uptake, R:

$$C_0 = -R\frac{r_0\,\delta_{eff.}}{3D_w} + C_\infty \quad (9)$$

By substitution of Eq. (9) into Eq. (7), the concentration at the radial distance, r, inside a sphere, which is surrounded by a *DBL*, is described by:

$$C_r = -\frac{R}{3}\left(\frac{r_0^2 - r^2}{2D_{agg.}} + \frac{r_0\,\delta_{eff.}}{D_w}\right) + C_\infty \quad (10)$$

where the concentration exactly at the center is

$$C_{r=0} = -\frac{R}{3}\left(\frac{r_0^2}{2D_{agg}} + \frac{r_0\,\delta_{eff.}}{D_w}\right) + C_\infty \quad (11)$$

which shows that the oxygen concentration at the center decreases proportionally to the volumetric respiration rate, to the product of the radius of the sphere and its DBL thickness, and to the square of the radius of the sphere, whereas it decreases inversely proportionally to the diffusion coefficients in the surrounding water and inside the aggregate.

Anoxic aggregates: When an anoxic central part is present in a sphere and thus all the oxygen is consumed close to the surface of the sphere, R can be described by:

$$R = \frac{4\pi r_0^2}{\frac{4}{3}\pi(r_0^3 - r_c^3)}\frac{D_w(C_\infty - C_0)}{\delta_{eff.}} \quad (12)$$

where r_c is the radial distance from the center at which the concentration of oxygen is zero, and

$$C_0 = -R\frac{\delta_{eff}(r_0 - r_c^3/r_0^2)}{3D_w} + C_\infty \quad (13)$$

Assuming zero order oxygen consumption, i.e. ignoring the small volume of the aggregate which follows first order kinetics (see 'Discussion'), C_r is described by:

$$C_r = -\frac{R}{3}\left(\frac{r_0^2 - r^2}{2D_{agg}} + \frac{\delta_{eff.}\,r_0}{D_w} - \frac{\delta_{eff}\,r_c^3/r_0^2}{D_w}\right) + C_\infty \quad (14)$$

where the respiration rate needed to create anoxia at the radial distance r_c within a sphere is described by:

$$R = 3C_\infty\left(\frac{r_0^2 - r_c^2}{2D_{agg.}} + \frac{\delta_{eff.}\,r_0}{D_w} - \frac{\delta_{eff.}\,r_c^3/r_0^2}{D_w}\right)^{-1} \quad (15)$$

Aggregates. Aggregates of detritus from a zooplankton culture, *Acartia tonsa*, which had been grown on *Rhodomonas baltica*, were made in roller tanks (Shanks & Edmonson 1989). The detritus included phytoplankton debris, fecal pellets and carcasses. The detritus was suspended in artificial seawater (hw Meersalz) of 30‰ with a pH of 8.2 in the roller tanks at 23°C. Eight aggregates were examined per day by the use of microelectrodes over a time period of 5 d.

Microelectrode measurements. Oxygen distributions were measured by a Clark-type oxygen microelectrode with a guard cathode (Revsbech 1989) mounted in a micromanipulator and calibrated in air-saturated and N_2-flushed seawater. The electrode current was measured by a picoammeter and read on a strip chart recorder. The tip diameter was 6 µm, the stirring sensitivity was <1%, and the 90% response time was 0.2 s. Sulfide was measured by a ~20 µm wide Ag/Ag_2S microelectrode, as described in Revsbech & Jørgensen (1986), connected to a mV-meter. The lower detection limit of sulfide was ~1 µM at pH 7.4 (Kühl & Jørgensen 1992). The pH microelectrodes were constructed ac-

cording to Revsbech & Jørgensen (1986). The pH sensing tip was ~20 µm in diameter and ~150 µm long. A calomel electrode was used as a reference, and the electrode potential was read on a mV-meter connected to a strip chart recorder. The electrode potential was calibrated in buffer solutions at pH 4.01, 7.00, and 9.21 (Ingold, Mettler Toledo Prozessanalytik).

The microelectrode measurements were done in a vertical net-jet flow system as described in Ploug & Jørgensen (unpubl.). The flow cell was built from 2 Plexiglas tubes (5 cm in diameter and 5 cm long). A nylon stocking was positioned between the 2 tubes which were glued together with silicon. The aggregates were kept freely suspended just above the net by an upward flow through a flow cell opposing their sinking velocities. The sinking velocities were calculated from the cross-sectional area of the flow cell and the volume of water flowing through the system per unit time. The position of the microelectrode relative to the surface of the aggregates was observed under a dissection microscope. All measurements were done at 23°C.

Data processing. The analytical solutions for the oxygen distributions in the DBL (cf. Eqs. 1 & 3) and within the aggregates (cf. Eqs. 12 & 14) were fitted to the measured values by applying the solver routine of the spreadsheet program Excel 4.0 (Microsoft). The volumetric respiration rate was expressed by Eqs. (11) and (13), whereby the model parameters were limited to r_c, r_0, r_∞ and the corresponding C_c, C_0, and C_∞. The $\delta_{eff.}$ was determined by the solver routine to yield the same flux as determined from the curvature of the oxygen profile in the DBL. In the solver routine, these model parameters were optimized to obtain a minimum value for the sum of the squares between the measured and the modeled oxygen concentrations. An effective diffusion coefficient inside aggregates similar to that in seawater (2.22×10^{-5} cm^2 s^{-1}) was assumed.

Detection of methanogenic bacteria. For DNA extraction, individual aggregates were transferred to 1.5 ml tubes with as little liquid as possible (500 to 600 µl) and centrifuged at 15800 × *g* for 10 min. The individual aggregates were resuspended in 110 µl sterile water (Sigma Chemical Co. Ltd) and 20 µl 10 × PCR (polymerase chain reaction) buffer [100 mM Tris-HCl (pH 9), 15 mM $MgCl_2$, 500 mM KCl, 0.1% (wt/vol) gelatin, 1% (vol/vol) Triton X-100] and subjected to repeated freeze thawing. The suspension was then mixed with 10 µl lysozyme (100 mg ml^{-1}) and incubated at 37°C for 1 h; 20 µl 200 mM DTT, 20 µl 0.01% (w/v) SDS (sodium dodecyl sulfate) and 20 µl Proteinase K (20 U ml^{-1}, 10 mg ml^{-1}) were added and incubated at 56°C for 1 h. The cell debris was pelleted by brief centrifugation, 0.1 to 5.0 µl of the supernatant was used for PCR amplification. DNA was also extracted from the following reference strains, which were obtained from the German Collection of Microorganisms (DSM, Braunschweig, Germany): *Escherichia coli* DSM 498, *Methanosarcina acetivorans* DSM 2834, *Methanolobus tindarius* DSM 2278 and *Methanobacterium formicicum* DSM 1535. Cells were collected from 50 ml cultures by centrifugation, resuspended in 1 ml TE buffer (50 mM Tris/HCl, 20 mM EDTA, pH 8) and subjected to repeated freeze thawing; 1 ml TE containing 5 mg ml^{-1} lysozyme was added to the suspension and incubated at 37°C for 30 min. The samples were further incubated at 56°C for 30 min after adding 100 µl 20% (w/v) SDS and 34 µl Proteinase K solution (20 U ml^{-1}) and sequentially extracted in phenol and phenol:chloroform:isoamyl alcohol (25:24:1). The aqueous extract was precipitated by adding 0.3 M sodium acetate, pH 7 (final concentration), and 2 volumes of ethanol. DNA was resuspended in 10 mM Tris/HCl containing 1 mM EDTA (pH 8).

PCR amplifications were performed with a Techne Cyclogene Temperature Cycler (Techne, Cambridge, UK) as follows: 0.1 to 5.0 µl of cell lysate or 10 to 100 ng of reference DNA, 50 pmol each of the appropriate primers, 25 nmol of each deoxyribonucleoside triphosphate, and 10 µl of 10 × PCR buffer were added to a 0.5 ml volume test tube, which was filled to a volume of 100 µl with sterile water and overlaid with 2 drops of mineral oil (Sigma Chemicals Co., Ltd). Primers complementary to conserved regions of the small subunit ribosomal RNA genes were used for PCR amplification. Primers 344F (archeal primer, 5'-ACGGGGYGCAGCAGGCGCGA-3'; Raskin et al. 1994) and 907R (universal primer, 5'-CCGTCAATTCMTTTGAGTTT-3', Lane 1991) were used for the amplification of archaeal 16S rDNA-fragments and primers 341F (bacterial primer, 5'-CCTACGGGAGGCAGCAG-3'; Lane 1991) and 907R were used for amplification of bacterial 16S rDNA fragments. To minimize non-specific annealing of the primers to nontarget DNA, SuperTaq DNA polymerase (HT Biotechnology, Ltd, Cambridge, UK) was added to the reaction mixture after the initial denaturing step (95°C, 5 min), at a temperature of 80°C. A 'touchdown' PCR (Don et al. 1991, Muyzer et al. 1995) was performed to increase the specificity of the amplification and to reduce the formation of spurious by-products. The annealing temperature was set 10°C above the expected annealing temperature (65°C) and decreased by 1°C every second cycle until a touchdown of 55°C, at which temperature 14 additional cycles were carried out. Samples were denatured at 95°C for 1 min, primer extension was carried out at 72°C for 3 min. After a final primer extension at 72°C for 10 min, the samples were incubated at 15°C. The amplification products were analyzed by electrophoresis in 2% (wt/vol) Seakem agarose (FMC) gels containing ethidium bromide (0.5 µg ml^{-1}).

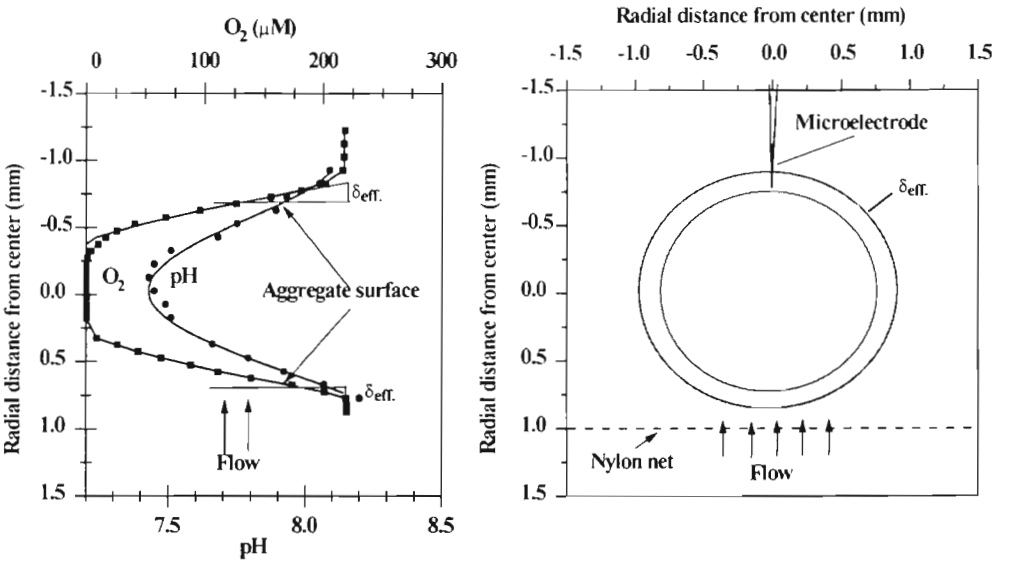

Fig. 2. Oxygen (■) and pH (●) distributions in a 1.4 mm large aggregate with a sinking velocity of 280 m d^{-1} The experimental conditions are shown

RESULTS

Anoxic aggregates

Anoxic conditions were detected in 2 out of 8 aggregates, only, on the second day of the experiment, although the surrounding water was fully oxygenated. There were no differences in the gradients measured in light and in darkness, which implies that no photosynthesis occurred in the aggregates under light conditions. An example of O_2 and pH gradients is shown in Fig. 2. The sinking velocity, being equal to the flow velocity, was 280 m d^{-1}. Anoxia was detected in a 0.40 mm wide zone in the aggregate, which had a diameter of 1.4 mm. The anoxic zone was slightly shifted to the rear of the aggregate because the $\delta_{eff.}$ was 0.05 mm upstream whereas the $\delta_{eff.}$ was 0.150 mm downstream. The pH gradients followed the oxygen gradients and it decreased by 0.76 pH units down to 7.44 in the center. No sulfide was, however, detectable with sulfide microelectrodes although the detection limit was ~1 µM. The decrease in pH was presumably only due to CO_2 release.

Molecular detection of methanogenic bacteria in anoxic aggregates

PCR amplification using the archaeal 16S rDNA primer combination 344F/907R was applied to examine anoxic aggregates for the presence of methanogenic bacteria. Primer 344F is a general archaeal primer which was shown to encompass most methanogenic and non-methanogenic archaea (Raskin et al. 1994). Amplification with primers 344F/907R yielded PCR products when template DNA extracted from the methanogenic reference strains *Methanosarcina acetivorans*, *Methanolobus tindarius* and *Methanobacterium formicicum* was used. However, no amplification products could be detected when different amounts (0.1 to 5.0 µl) of template DNA from the aggregates or the γ-Proteobacterium *Escherichia coli* were used. Using the bacterial 16S rDNA primer combination 341F/907R, PCR products were obtained with *E. coli* template DNA as well as with 0.1 µl and 1.0 µl of aggregate DNA. 16S rDNA fragments were not amplified when template DNA from the methanogenic reference strains was used. These results demonstrate that the amplification reaction using primer combination 344F/907R or 341F/907R was specific for archaea or bacteria, respectively. The bacterial 16S rDNA PCR products which were amplified from aggregate DNA indicate that bacteria were present in the aggregates. In contrast, archaeal sequences could not be detected in the anoxic aggregates, suggesting that methanogenic bacteria were not present.

Respiration

The volumetric oxygen respiration rate around an anoxic center in a 1.4 mm large aggregate (Fig. 2) was calculated as 22.1 nmol O_2 mm^{-3} h^{-1} (cf. Eqs. 12 & 15). The volumetric oxygen respiration rates were calculated from the profiles measured in 8 aggregates d^{-1} over 5 d (Fig. 3). The mean diameter of the shortest axis of the aggregates was 1.02 ± 0.29 mm, whereas the mean diameter of the longest axis was 1.77 ± 0.84 mm, and the sinking rates ranged from 82 to 314 m d^{-1}. The oxygen respiration showed an exponential decrease over time, indicating that oxygen respiration was carbon limited. The $T_{1/2}$ was 2.3 d.

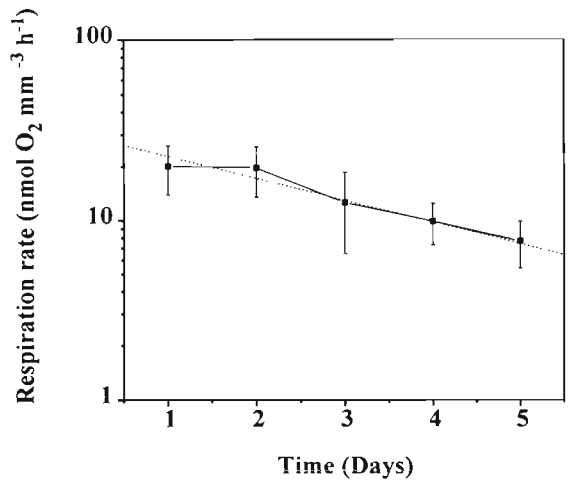

Fig. 3. Volumetric oxygen respiration rate in sinking aggregates measured over 5 d. Bars: standard deviation of the mean (n = 8). Dotted line: a linear regression through the measured values

Three examples of the oxygen distributions measured in the DBL and inside the aggregates with different volumetric oxygen respiration rates are shown (Fig. 4). The oxygen distribution in and around the aggregates could be modeled using an effective diffusion coefficient inside the aggregates similar to that in seawater, which was 2.23×10^{-5} cm^2 s^{-1} at 23°C (Broecker & Peng 1974). The curves (Fig. 4) represent the modeled oxygen distributions in a 1 mm sphere at the different volumetric oxygen respiration rates. At an oxygen respiration rate of 20 nmol O_2 mm^{-3} h^{-1}, corresponding to the mean oxygen respiration rate at Day 1 (Fig. 3), the oxygen concentration in the center was still 60 µM or 27% of the air-saturated water phase, whereas the oxygen concentration in the center was 82% of the air-saturated water phase when the oxygen respiration rate was 6 nmol O_2 mm^{-3} h^{-1}, corresponding to the mean respiration rate at Day 5. The oxygen concentrations measured in the center in non-anoxic aggregates at different oxygen respiration rates are shown in Fig. 5. The corresponding theoretical oxygen concentrations in the center (cf. Eq. 11) are also shown in the case of an infinite DBL ($\delta_{eff.} = r_0$) and with no DBL. The measured DBL thickness, $\delta_{eff.}$, was 0.16 ± 0.29 mm upstream and 0.19 ± 0.16 mm downstream. The resistance in the DBL lowered the oxygen respiration rate necessary to create anoxia at the very center of a 1 mm spherical aggregate by 33%, i.e. from 42 to 28 nmol O_2 mm^{-3} h^{-1}. The DBL was, thus, of high significance for mass transfer resistance and oxygen depletion inside such small aggregates.

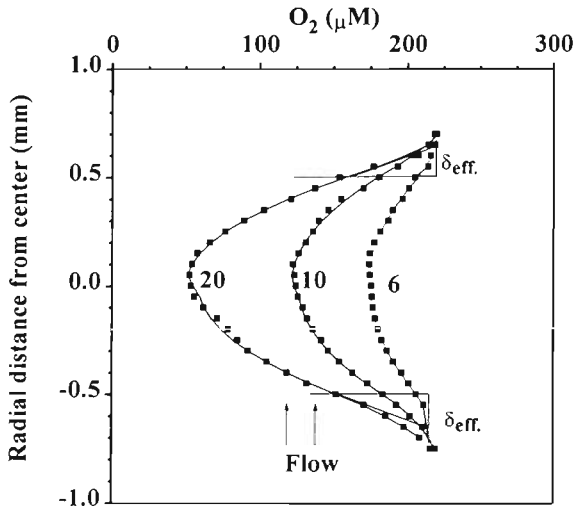

Fig. 4. Measured (■) and modeled (solid curves) oxygen distributions at different volumetric oxygen respiration rates indicated by the number on the curves (in nmol O_2 mm^{-3} h^{-1}). Effective DBL thickness, $\delta_{eff.}$, and aggregate surface are indicated

Anoxia and degradation time

Anoxia in the center of an aggregate is dependent on the relative importance of advection to diffusion, the volumetric respiration rates, the size of the aggregate and the bulk water concentration of oxygen (cf. Eq. 11). The oxygen respiration rate necessary to create anoxia exactly at the center of spheres of different sizes was calculated theoretically for spherical diffusion, a bulk water concentration of 250 µM, a molecular diffusion coefficient of O_2 in the aggregates similar to that in seawater (2.23×10^{-5} cm^2 s^{-1}), and an evenly distributed

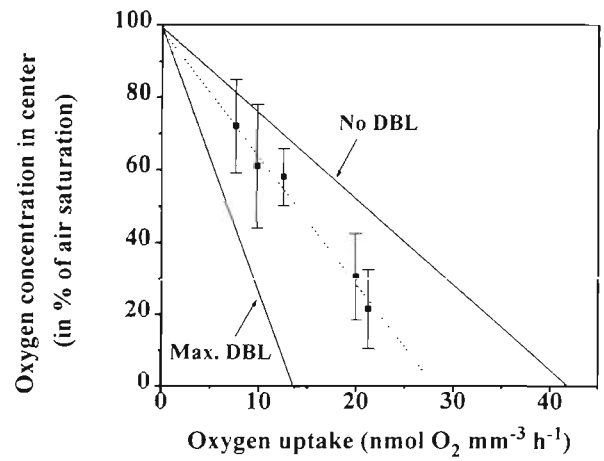

Fig. 5. Measured oxygen concentration (mean ± SD, n = 6 to 8) in the center of non-anoxic aggregates with a mean size of 1 mm at different volumetric oxygen respiration rates. Modeled oxygen concentration in the center with a maximum DBL thickness and no DBL is indicated

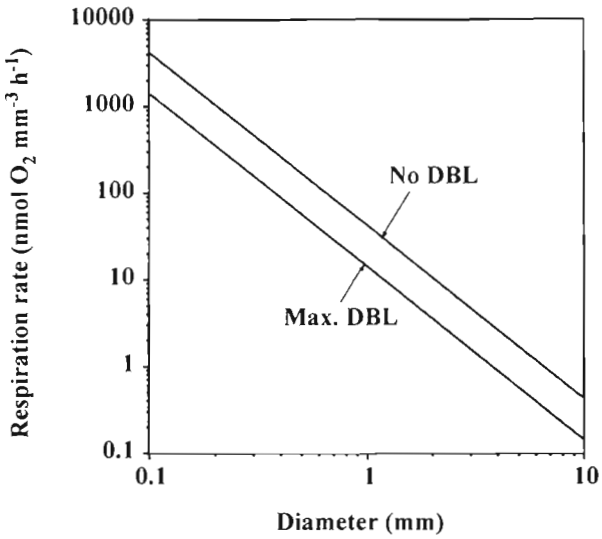

Fig. 6. Volumetric oxygen respiration rates required to create anoxic conditions exactly in the center of an aggregate (shaded area) with a DBL ranging from maximal to minimal thickness

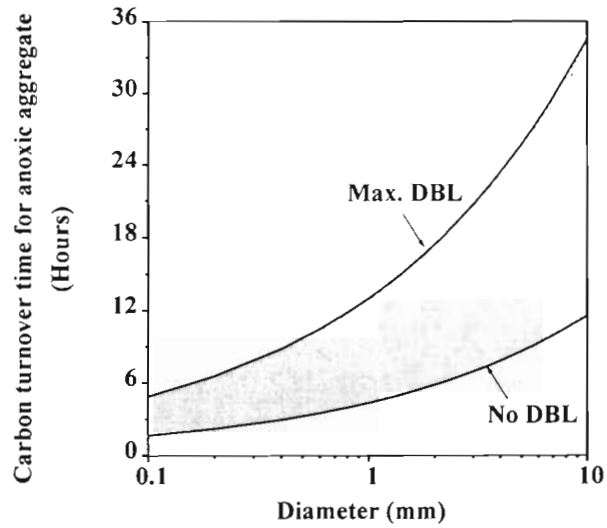

Fig. 7. Calculated carbon turnover time in marine anoxic aggregates (shaded area) with a DBL ranging from maximal to minimal thickness (see text)

respiration inside the spheres. This was done assuming an infinite DBL thickness ($\delta_{eff.} = r_0$), or assuming no DBL at the aggregate-water interface (cf. Eq. 11) (Fig. 6). As the radius decreases 10-fold, the oxygen respiration rate necessary to create anoxia exactly at the center increases 100-fold. Thus, for an anoxic aggregate with a diameter of 100 µm the oxygen respiration rate required would be 1400 to 4200 nmol mm^{-3} h^{-1}, whereas for large 1 cm aggregates an oxygen respiration rate of 0.14 to 0.42 nmol mm^{-3} h^{-1} could theoretically create anoxia in the center if mass transfer occurs only by molecular diffusion.

The carbon turnover time for anoxic aggregates which are anoxic at the very center was calculated from reported size-dependent dry weights and volumes of natural aggregates in the ocean (Alldredge & Gotschalk 1988). The POC was here assumed to be 20% of dry weight densities (Alldredge 1979) and the respiratory quotient was assumed to be 1. According to these calculations the carbon turnover time would range from 1.5 to 34 h for anoxic aggregate sizes ranging from 0.01 to 1 cm, respectively, depending on the DBL thickness (Fig. 7). Small anoxic aggregates or fecal pellets will therefore be degraded very rapidly in the ocean, and anoxia will only persist for a relatively short period of time. Under diffusion limitation, i.e. anoxic conditions inside the aggregates, the carbon turnover time is inversely proportional to the oxygen concentration in the surrounding waters. Anoxic aggregates may, therefore, prevail in an oxygen minimum zone in the ocean. With an oxygen concentration of 10% of air saturation, anoxic conditions in aggregates will be prolonged to occur for several days up to perhaps weeks.

DISCUSSION

DBLs develop where the eddy diffusion coefficient becomes smaller than the molecular diffusion coefficient, because at small scale and at interfaces the water movement is dominated by viscous forces, and molecular diffusion is fast relative to advective flow. The aggregates investigated here were composed of detritus from a zooplankton culture and included phytoplankton debris, fecal pellets and carcasses. The aggregates appeared very dense and compact, which was also reflected in their relatively high sinking velocities, ranging from 82 to 314 m d^{-1}. Gradients of oxygen and pH occurred inside the aggregates and in the DBL surrounding the aggregates. The oxygen gradients could be described by simple molecular diffusion models. Advection was, thus, presumably limited inside the aggregates.

The mean effective DBL, δ_{eff}, of 1 mm large aggregates was 0.17 mm thick. The boundary layer thickness is dependent on shear induced by sinking as well as on turbulence in the environment. The Sherwood number, *Sh*, for oxygen transfer to a sphere which sinks in a turbulent environment can be described by (Batchelor 1980, see also Karp-Boss et al. 1996):

$$Sh = 0.52\left[2.25\left(\frac{r_0 U}{D}\right)^2 + 1.84\left(\frac{r_0^2}{D}\sqrt{\frac{\varepsilon}{\nu}}\right)^2\right]^{1/6} \quad (16)$$

or

$$Sh = 0.52[2.25(Pe_{sinking})^2 + 1.84(Pe_{turbulence})^2]^{1/6}$$

where r_0 is the radius, U is the sinking velocity, D is the

diffusion coefficient, ε is the energy dissipation rate and ν is the kinematic viscosity of sea water; $\sqrt{\varepsilon/\nu}$ is the turbulent shear rate, E (s^{-1}). *Pe* is the Peclet number. The equation is valid for $Pe \gg 1$. In the surface waters of the ocean the shear rate normally ranges from 0.1 to 1.0 s^{-1} (MacKenzie & Leggett 1991). In the presence of turbulence with a shear rate of 1.0 s^{-1}, *Sh* ranges from 2.77 at neutral buoyancy to 4.59 for a 1 mm sinking sphere (170 m d^{-1}) (cf. Eq. 14). These Sherwood numbers correspond to a δ_{eff} of 0.18 to 0.11 mm (cf. Eq. 6), which is close to the measured δ_{eff} of 0.17 mm.

The measured profiles in the aggregates of the present study could be well described by the theoretical distributions of oxygen in a sphere assuming a diffusion coefficient of O_2 inside the aggregates similar to that in seawater and an evenly distributed respiration of zero order (Fig. 4). The molecular diffusion coefficient of O_2 in mucus produced by the colony forming microalgae *Phaeocystis* sp. has recently been experimentally shown to be similar to that in seawater (H. Ploug, W. Stolte, E. H. G. Epping & B. B. Jørgensen unpubl.). A diffusion coefficient of O_2 inside marine aggregates similar to that in seawater may therefore be expected as well. A lower diffusion coefficient in the aggregates would imply steeper gradients of oxygen inside the aggregates. As the spatial resolution of oxygen measurements by microelectrodes is the same as the tip diameter, e.g. 6 µm, and the 90% response time was 0.2 s, anoxic 'microzones' with dimensions <100 µm, e.g. formed due to a locally lower diffusion coefficient in marine aggregates, would in principle be detectable with the microelectrode technique unless surrounded by a protecting wall. We did not detect such microzones in the present study.

The calculations of the oxygen consumption rates were done assuming zero order kinetics. The half-saturation constant, K_m, for oxygen respiration is approximately 1 µM in heterotrophic microorganisms (Focht & Verstraete 1977). An anoxic center in an aggregate being immersed in oxygenated water implies very steep oxygen gradients within the DBL and inside the aggregate. The fraction of the aggregate (Fig. 2) in which respiration presumably was oxygen limited was very small, i.e. the anoxic zone of the aggregate comprised ca 8% of the total aggregate volume. The zone in which O_2 was present at concentrations <10 µM (10-fold K_m) and, thus, presumably followed first order kinetics was found at the radial distance $0.225 < r < 0.350$ mm, which comprised <9% of the total aggregate volume, assuming spherical geometry. The error in the calculated respiration rates introduced by assuming zero order kinetics was accordingly <9%.

The mass transfer resistance in the DBL surrounding the aggregates with a mean size of 1 mm lowered the oxygen respiration required to create anoxic conditions by 33%. The lower limit for the oxygen respiration rate needed to create anoxia at the center of 1 mm large aggregates was found at 28 nmol O_2 mm^{-3} h^{-1} (Fig. 5). Anoxia was only detected in the largest aggregates, and a 0.4 mm wide zone with anoxic conditions was measured early in the degradation process of a 1.4 mm aggregate with a volumetric oxygen respiration rate of 22.1 nmol O_2 mm^{-3} h^{-1} (Fig. 2). With a respiratory quotient of 1, carbon must be degraded at the same rate, and such anoxic microenvironments may therefore rapidly become carbon limited.

Hansen & Bech (1996) found that fecal pellets of the copepod *Acartia tonsa* are mainly colonized by bacterioplankton from the surrounding waters, and the bacterial numbers associated with fecal pellets were stable after 150 h (Hansen et al. 1996). The exponential decay of oxygen respiration rate in the aggregates of the present study (Fig. 3) with a $T_{1/2}$ of 2.3 d indicates that the oxygen respiration rates in these aggregates were carbon limited and not limited by e.g. sub-optimal colonization by microorganisms. Studies of the bacterial colonization and carbon degradation of fecal pellets from *A. tonsa* cultures have also shown an immediate exponential decay of fecal pellets with $T_{1/2}$ ranging between 0.09 and 17.2 d at 18°C (Lee & Fisher 1992a, Hansen et al. 1996). The observed half-time of respiration in the present study was, thus, within the same range as observed for decomposition of zooplankton debris at similar temperature. $T_{1/2}$ for phyto- and zooplankton debris is up to 100-fold longer at 2 to 4°C, which may be due to lower bacterial respiration and growth rates (Lee & Fisher 1992, 1993). Anoxic aggregates harboring methanogenic bacteria may therefore not be expected during algal blooms at low temperature. A previous study on the microbial population structure of marine phytodetrital macroaggregates comprised of diatoms and *Phaeocystis* colonies, being typical during algal blooms, showed that archaeal DNA and RNA were not associated with such aggregates (DeLong et al. 1993). Microelectrode studies in *Phaeocystis* colonies have also shown 50-fold lower respiration rates as compared to the present study, whereby such colonies very unlikely become anoxic (Ploug et al. unpubl.).

DBLs and anoxia have been measured in a several millimeter large crustacean fecal pellet attached to a particle of marine snow (Alldredge & Cohen 1987). Copepod fecal pellets are, however, significantly smaller with a long axis ranging from 88 to 168 µm, while the short axis is approximately 40 µm (Hansen et al. 1996). Depending on the DBL thickness, anoxic conditions in a 'spherical' fecal pellet with a diameter of 70 µm would require an oxygen respiration rate of 3.2 to 9.8×10^3 nmol O_2 mm^{-3} h^{-1}, assuming a diffusion coefficient of O_2 similar to that in seawater. The carbon

content of fecal pellets produced by copepods is approximately 0.060 pg C μm^{-3}, equal to 5.0 µmol C mm^{-3} (Gonzales & Smetacek 1994). Anoxic conditions occurring only at the very center would accordingly predict a carbon turnover time of 0.06 d assuming spherical geometry, maximal DBL thickness, and a diffusion coefficient similar to that in seawater, and require a 100% remineralization to CO_2. With an observed $T_{1/2}$ of 0.09 to 17.2 d (Lee & Fisher 1992a, Hansen et al. 1996) for fecal pellets which also release DOC, such small fecal pellets would not be anoxic. Anoxic conditions in such fecal pellets with a volumetric oxygen respiration rate of 22.1 nmol O_2 mm^{-3} h^{-1}, i.e. the highest measured in the present study, would require a diffusion coefficient 100-fold less than that of seawater or alternatively that pO_2 of the surrounding water is reduced down to 1% of air saturation.

The diffusion distance of oxygen and the accumulation of organic matter are both highly increased when fecal pellets are trapped in marine snow. Thereby anoxic conditions are more likely to occur as the oxygen respiration rate necessary to create anoxic conditions decreases 100-fold as the radius increases 10-fold (Fig. 6). The calculated turnover times of carbon required to generate an anoxic center in marine aggregates with sizes ranging from 100 µm to 1 cm were in the order of 1.5 to 34 h (Fig. 7). As the degradation process becomes carbon limited, the oxygen consumption rate will decrease as the carbon is consumed and remineralized or released as DOC. Because anoxia will prevail only until the respiration becomes carbon limited, the calculated time range represents a maximum estimate of the turnover time of anoxic aggregates. Advective transport of oxygen inside large porous aggregates will enhance the availability of oxygen and, thus, decrease the carbon turnover time of large anoxic aggregates as here calculated, assuming molecular diffusion as the only mass transfer process. The sinking velocity and the porosity of the aggregates increase with size (Alldredge & Gotschalk 1988), and advective transport oxygen may therefore be more important for mass transfer in several mm to cm large aggregates (Logan & Alldredge 1989). Carbon turnover times in marine snow have earlier been estimated from bacterial production rates (Simon et al. 1990, Smith et al. 1992). These studies showed carbon turnover times ranging from 20 to 1429 d. These degradation rates were, thus, 10- to 1000-fold lower than the respiratory rates necessary to create anoxic conditions. Intense hydrolysis of particulate amino acids by bacterial ectoenzymes have shown turnover times of 0.2 to 2.1 d for such pools with very little of the hydrolysate being taken up by the attached bacteria in marine aggregates, whereby the nutritional value of marine aggregates rapidly decreases (Smith et al. 1992).

In situ measurements of methane fluxes from sediment trap material have suggested that methanogenic bacteria are associated with sinking particulate matter (Karl & Tilbrook 1994). The exact source of methane accumulating in the traps could, however, not be determined (Tilbrook & Karl 1995). Nitrification and methanogenesis have earlier been measured in sediment trap material composed of detritus and fecal pellets in the size range of 43 to 150 µm (Bianchi et al. 1992). Methanogenic activity associated with sediment trap material including such fecal pellets was, however, only detectable after long incubation times of 30 to 40 d under anaerobic conditions (Bianchi et al. 1992, Marty 1993). By the use of archaeal-specific primers we did not detect any methanogenic bacteria in the anoxic aggregates. The ephemeral anoxic state and the very dynamic change of the oxygen microenvironment in the aggregates suggest that such microenvironments are too unstable for the relatively slow growth of obligatory anaerobic bacteria such as methanogenic and sulfate-reducing bacteria, and it may explain why neither archea nor sulfide was detected inside the aggregates. Only bacteria and other microorganisms that can grow over a wide range of oxygen concentration and pH may efficiently exploit such a microenvironment rich in carbon and nutrients.

As shown in the present study, stable anoxic conditions require a high and continuous carbon supply to support the oxygen consumption rates. The methane and sulfide production observed in oxygenated waters may be due to zooplankton grazing as previously suggested by De Angelis & Lee (1994) and it is most likely produced in meso- and/or macrozooplankton guts. A continuous passage and degradation of organic matter and/or a strong diffusive barrier for O_2 is required to provide stable anoxic conditions, where methanogenic bacteria can grow.

Acknowledgements. Detritus from *Acartia tonsa* cultures was kindly provided by Thomas Kiørboe. We thank Eric H. G. Epping for developing the computer analysis software. Cindy Lee is thanked for discussions. Microelectrodes were constructed by Anja Eggers and Gaby Eickert at the Max Planck Institute. This work was supported by the Danish Natural Science Research Council (J: 11-0557-1 to H.P.), the Danish Research Academy (J: V930148 to H.P.), and by the Max Planck Gesellschaft (Germany).

LITERATURE CITED

Alldredge AL (1979) The chemical composition of macroscopic aggregates in two neretic seas. Limnol Oceanogr 24:855–866

Alldredge AL, Cohen Y (1987) Can microscale chemical patches persist in the sea? Microelectrode study of marine snow and fecal pellets. Science 235:689–691

Alldredge AL, Gotschalk C (1988) In situ settling behavior of marine snow. Limnol Oceanogr 33(3):339–351
Alldredge AL, Silver M (1988) Characteristics, dynamics and significance of marine snow. Prog Oceanogr 20:41–82
Batchelor GK (1980) Mass transfer from small particles suspended in turbulent fluid. J Fluid Mech 98:609–623
Bianchi M, Marthy D, Teyssié JL, Fowler SW (1992) Strictly aerobic and anaerobic bacteria associated with sinking particulate matter and zooplankton fecal pellets. Mar Ecol Prog Ser 88:55–60
Biddanda BA (1988) Microbial aggregation and degradation of phytoplankton-derived detritus in seawater. II. Microbial metabolism. Mar Ecol Prog Ser 42:89–95
Biddanda BA, Pomeroy LR (1988) Microbial aggregation and degradation of phytoplankton-derived detritus in seawater. I. Microbial succession. Mar Ecol Prog Ser 42:79–88
Broecker WS, Peng TH (1974) Gas exchange rates between air and sea. Tellus 26:21–35
Crank J (1975) The mathematics of diffusion. Oxford University Press, Oxford
De Angelis MA, Lee C (1994) Methane production during zooplankton grazing on marine phytoplankton. Limnol Oceanogr 39:1298–1308
DeLong EF, Franks DG, Alldredge AL (1993) Phylogenetic diversity of aggregate-attached vs. free-living marine bacterial assemblages. Limnol Oceanogr 38:924–934
Don RH, Cox PT, Wainwright BJ, Baker K, Mattick JS (1991) 'Touchdown' PCR to circumvent spurious priming during gene amplification. Nucl Acids Res 19:4998
Focht DD, Verstraete W (1997) Biochemical ecology of nitrification and denitrification. Adv Microbiol Ecol 1: 135–214
Gonzales HE, Smetacek V (1994) The possible role of the cyclopoid copepod *Oithona* in retarding vertical flux of zooplankton faecal material. Mar Ecol Prog Ser 113: 233–246
Hansen B, Bech G (1996) Bacteria associated with marine planktonic copepod in culture. I. Bacterial genera in seawater, body surface, intestines and fecal pellets and succession during fecal pellet degradation. J Plankton Res 18: 257–273
Hansen B, Fotel FL, Jensen NJ, Madsen SD (1996) Bacteria associated with a marine planktonic copepod in culture. II. Degradation of fecal pellets produced on a diatom, a nanoflagellate or a dinoflagellate diet. J Plankton Res 18: 275–288
Jørgensen BB (1977) Bacterial sulfate reduction within reduced microniches of oxidized marine sediments. Mar Biol 41:7–17
Karl DM, Tilbrook BD (1994) Production and transport of methane in oceanic particulate organic matter. Nature 368:732–734
Karp-Boss L, Boss E, Jumars PA (1996) Nutrient fluxes to planktonic osmotrophs in the presence of fluid motion. Oceanogr Mar Biol Ann Rev 34:71–107
Kühl M, Jørgensen BB (1992) Microsensor measurements of sulfate reduction and sulfide oxidation in compact microbial communities of aerobic biofilms. Appl Environ Microbiol 58:1164–1174
Lamontagne RA, Swinnerton JW, Linnebom VJ, Smith WD (1973) Methane concentrations in various marine environments. J Geophys Res 78:5317–5324
Lane DJ (1991) 16S/23S rRNA Sequencing. In: Stackebrandt E, Goodfellow M (eds) Nucleic acid techniques in bacterial systematics. John Wiley & Sons Ltd, Chichester, p 115–175
Lee BG, Fisher NS (1992a) Decomposition and release of elements from zooplankton debris. Mar Ecol Prog Ser 88: 117–128
Lee BG, Fisher NS (1992b) Degradation and elemental release from phytoplankton debris and their geochemical implications. Limnol Oceanogr 37:1345–1360
Lee BG, Fisher NS (1993) Release of trace elements and protein from decomposing planktonic debris. 1. Phytoplankton debris. J Mar Res 51:391–421
Logan BE, Alldredge AL (1989) Potential for increased nutrient uptake by flocculating diatoms. Mar Biol 101:443–450
MacKenzie BR, Leggett WC (1991) Quantifying the contribution of small-scale turbulence to the encounter rates between larval fish and their zooplankton prey: effect of wind and tide. Mar Ecol Prog Ser 73:149–160
Marty DG (1993) Methanogenic bacteria in seawater. Limnol Oceanogr 38:452–456
Muyzer G, Hottenträger S, Teske A, Wawer C (1995) Denaturing gradient gel electrophoresis of PCR-amplified 16S rDNA. A new molecular approach to analyse the genetic diversity of mixed microbial communities. In: Akkermans ADL, Van Elsas JD, De Bruijn FJ (eds) Molecular microbial ecology manual, 2nd edn. Kluwer, Dordrecht, p 1–22
Raskin L, Stromley JM, Rittmann BE, Stahl DA (1994) Group-specific 16S rRNA hybridization probes to describe natural communities of methanogens. Appl Environ Microbiol 60: 1232–1240
Revsbech NP (1989) An oxygen microelectrode with a guard cathode. Limnol Oceanogr 34: 474–478
Revsbech NP, Jørgensen BB (1986) Microelectrodes: their use in microbial ecology In: Marshall KC (ed) Advances in microbial ecology, Vol 9. Plenum, New York, p 293–352
Shanks AL, Edmonson EW (1989) Laboratory-made artificial marine snow: a biological model of the real thing. Mar Biol 101:463–470
Shanks AL, Reeder ML (1993) Reducing microzones and sulfide production in marine snow. Mar Ecol Prog Ser 96:43–47
Sherwood TK, Pigford RL, Wilke CR (1975) Mass transfer. McGraw-Hill Book Company
Sieburth J McN (1993) C_1 bacteria in the water column of Chesapeake Bay, USA. I. Distribution of sub-populations of O_2-tolerant, obligatory anaerobic, methylotrophic methanogens that occur in microniches reduced by their bacterial consorts. Mar Ecol Prog Ser 95:67–80
Simon M, Alldredge AL, Azam F (1990) Bacterial carbon dynamics on marine snow. Mar Ecol Prog Ser 65:205–211
Smith DC, Simon M, Alldredge AL, Azam F (1992) Intense hydrolytic enzyme activity on marine aggregates and implications for rapid particle dissolution. Nature 359:139–142
Tilbrook BD, Karl DM (1995) Methane sources, distributions and sinks from California coastal waters to the oligotrophic North Pacific gyre. Mar Chem 49:51–64

Responsible Subject Editor: Tom Fenchel, Helsingør, Denmark

Manuscript received: December 22, 1996
Revised version accepted: June 14, 1997